



# Measurement report: Greenhouse gas profiles and age of air from the 2021 HEMERA-TWIN balloon launch

Tanja J. Schuck<sup>1</sup>, Johannes Degen<sup>1</sup>, Timo Keber<sup>1</sup>, Katharina Meixner<sup>1</sup>, Thomas Wagenhäuser<sup>1</sup>, Mélanie Ghysels<sup>2</sup>, Georges Durry<sup>2</sup>, Nadir Amarouche<sup>3</sup>, Alessandro Zanchetta<sup>4</sup>, Steven van Heuven<sup>4</sup>, Huilin Chen<sup>4,7</sup>, Johannes C. Laube<sup>5</sup>, Sophie L. Baartman<sup>6,\*</sup>, Carina van der Veen<sup>6</sup>, Maria Elena Popa<sup>6</sup>, and Andreas Engel<sup>1</sup>

<sup>1</sup>Institute for Atmospheric and Environmental Sciences, University of Frankfurt, Frankfurt, Germany

<sup>2</sup>Groupe de Spectrométrie Moléculaire et Atmosphérique, Université de Reims, France

<sup>3</sup>Institut National des Sciences de l'Univers Division Technique, Meudon, France

<sup>4</sup>Centre for Isotope Research, University of Groningen, The Netherlands

<sup>5</sup>Institute of Climate and Energy Systems: Stratosphere (ICE-4), Jülich Research Centre, Germany

<sup>6</sup>Institute for Marine and Atmospheric research Utrecht, Utrecht University, The Netherlands

<sup>7</sup>The School of Atmospheric Sciences, Nanjing University, China

\* now at Meteorology and Air Quality Group, Wageningen University and Research Centre, The Netherlands

**Correspondence:** Tanja J. Schuck (schuck@iau.uni-frankfurt.de)

## Abstract.

Within the HEMERA balloon infrastructure project, a stratospheric balloon carrying a multi-instrument payload to a maximum altitude of 31.2 km was launched on 12th August 2021. Aboard the openly constructed TWIN gondola, several types of instruments were used for simultaneous air sampling and in-flight measurements to characterize climate relevant trace gases in the stratosphere and in the troposphere, and to compare and evaluate different instrumental approaches and sampling techniques. For observations of the main greenhouse gases carbon dioxide (CO<sub>2</sub>), methane (CH<sub>4</sub>), nitrous oxide (N<sub>2</sub>O) and sulfur hexafluoride (SF<sub>6</sub>), sampling with AirCores, flask sampling and in-flight spectrometry were deployed. Overall, results from different methods agree well. While better precision is achieved for the post-flight measurements of AirCores and flask sampling, in-situ spectrometry provides a higher degree of detail on the vertical structure of the CH<sub>4</sub> profile. Age of air was derived from mixing ratios of CO<sub>2</sub> and SF<sub>6</sub>. As seen in previous studies, higher values were obtained from SF<sub>6</sub> than from CO<sub>2</sub>. Correcting for chemical losses, maximum values of 4.4–5.1 years were derived from SF<sub>6</sub> mixing ratios at altitudes above 20 km compared to 4.2–5.0 years from CO<sub>2</sub> mixing ratios. The resulting dataset should be well suited for multi-tracer approaches to derive age of air, in particular in combination with a large suite of halocarbons measured from flask samples and one more AirCore which are reported by a companion publication.

## 15 1 Introduction

High-altitude balloons continue to be the only means for in-situ observations of chemical composition at altitudes that cannot be reached by aircraft, i.e. above ca. 20 km. Such data are for example relevant to constrain potential changes in stratospheric circulation induced by climate change (Austin and Li, 2006; Engel et al., 2009; Stiller et al., 2012; Eichinger et al., 2019; Aba-



los et al., 2021). It is also of interest to perform measurements of ozone depleting gases directly at the altitudes where ozone depletion occurs (Ray et al., 2002; Brinckmann et al., 2012; Krysztofiak et al., 2023). For substances which are measurable with remote-sensing methods, data from balloon-borne air samples can also be used for satellite retrieval validation or to supplement ground-based measurement networks such as the Total Carbon Column Observing Network (TCCON) and the Network for the Detection of Atmospheric Composition Change (NDACC) deploying Fourier transform infrared spectrometers (Zhou et al., 2018). This was for example recently demonstrated for vertical profiles of HCFC-22 (Chlorodifluoromethane,  $\text{CHClF}_2$ ) measured by the ACE-FTS satellite instrument (Kolonjari et al., 2024). However, due to the high costs and safety aspects of such launches, profiles from large high-altitude balloons remain sparse in their spatial and temporal coverage (Krysztofiak et al., 2023; Ray et al., 2024).

Over the last decade, air sampling with AirCores, based on an idea initially proposed by Tans (2009), has been established as a method for measurements of vertical profiles of  $\text{CO}_2$  and  $\text{CH}_4$  (Karion et al., 2010; Membrive et al., 2017; Engel et al., 2017; Wagenhäuser et al., 2021). AirCores are a lightweight air sampling tool based on stainless steel tubes that are open at one end and closed at the other. Making use of the pressure changes with altitude, air is passively sampled into the tube during the descent from high altitudes to the ground. They are often sufficiently lightweight to be carried by small weather balloons. This approach is complementary to classical flask sample collection at distinct altitudes. While the latter averages over few well-defined sampling intervals, AirCores provide a continuous profile. AirCore samples need to be analysed quickly after sampling to minimize the averaging effects of molecular diffusion within the sample tube and to achieve the best possible vertical resolution. Also, sub-sampling of AirCores for later analysis using discontinuous analytical methods - at the expense of losing altitude resolution - is possible (Laube et al., 2020). Sub-sampled AirCore samples, as original flask samples, can be analysed for many species even after longer times of storage, depending on the chemical stability of compounds in the flasks. The 2021 launch of the HEMERA-TWIN gondola described in this measurement report allowed the simultaneous deployment of several AirCore packages for inter-comparison of different AirCores and for comparison with reference methods, which is not possible with small weather balloons because of their payload weight restrictions.

To investigate stratospheric transport time scales, the concept of mean age of air has proven to be a useful tool (Hall and Plumb, 1994; Waugh and Hall, 2002; Engel et al., 2009). Commonly, the mean age of air is interpreted as the mean transit time that it took for all contributions to an observed air parcel to arrive at the observation location from their respective entry points into the stratosphere. The calculation relies on a reference time series of mixing ratios measured at a reference surface. Often, the tropical tropopause is chosen as the reference surface. For the lower stratosphere of the mid latitudes, more sophisticated approaches take into account cross-tropopause transport in the extra-tropics as well (Hauck et al., 2020; Wagenhäuser et al., 2023; Ray et al., 2024). Generally, the stratospheric age of air can be calculated from observations of long-lived trace gases which have a monotonous trend in the troposphere, for example  $\text{SF}_6$  or, when de-seasonalised,  $\text{CO}_2$  (Volk et al., 1997; Engel et al., 2002; Bönisch et al., 2009; Ray et al., 2014; Engel et al., 2017; Garny et al., 2024a; Ray et al., 2024). Also halocarbons have been used to derive age of air (Leedham Elvidge et al., 2018). Age of air values need to be corrected for the acceleration of tropospheric trends, as trace gas mixing ratios in general show non-linear trends (Plumb and Ko, 1992; Volk et al., 1997; Engel et al., 2002). In addition, the chemical sinks of  $\text{SF}_6$  may introduce significant biases to the calculation (Stiller et al., 2012;

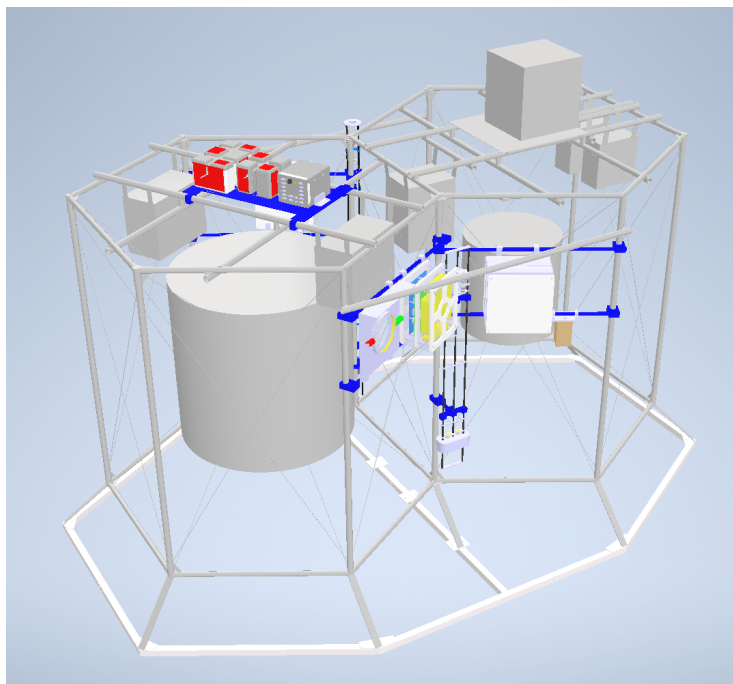


**Figure 1.** Layout of the TWIN gondola for the HEMERA 2021 launch. The gondola height is 2.2 m, footprint is 2.6 m x 4 m, and the total weight including the instrumentation amounts to approximately 345 kg.

Ray et al., 2017; Kovács et al., 2017; Leedham Elvidge et al., 2018). Recently, Garny et al. (2024a) proposed a model-based  
55 correction scheme to account for chemical sinks of SF<sub>6</sub>. For CO<sub>2</sub>, also the seasonal cycle in the troposphere needs to be taken  
into account at least in the lower stratosphere (Bönisch et al., 2009; Andrews et al., 2001; Diallo et al., 2017).

Here, we report on the HEMERA-TWIN balloon launch of 2021 which aimed at sampling and analysing stratospheric air  
to measure atmospheric trace gases using four types of instruments: cryogenic air sample collection in stainless steel canisters,  
bag sampling, air sampling by means of AirCores and in-situ spectrometric analysis. This combination of instruments allows to  
60 compare vertical profiles of the long-lived greenhouse gases CO<sub>2</sub>, CH<sub>4</sub>, SF<sub>6</sub> and N<sub>2</sub>O measured at different altitude resolution  
and of the mean age of air derived from SF<sub>6</sub> and CO<sub>2</sub>. As discussed in our companion paper, the collection of air samples  
provides additional data on mixing ratios of halocarbons, many of them being strong greenhouse gases and ozone depleting  
substances (Laube et al., 2024).



## 2 Methodology

### 65 2.1 The HEMERA-TWIN balloon launch

HEMERA is a balloon infrastructure project offering balloon flights for research and innovation. It is funded by the European Commission within the Horizon 2020 program and is coordinated by the French space agency CNES (Centre National d'Etudes Spatiales). In August 2021, the openly constructed TWIN gondola shown in Fig. 1 was used as part of the HEMERA flight programme to carry a suite of instruments to measure the vertical distribution of several long lived greenhouse gases and ozone-depleting substances. The TWIN gondola has been used before in similar studies and is known to be suited for whole air sampling without contamination of the sampled air (Engel and Schmidt, 1994). The open structure avoids contact of the sampled air with surfaces and thus reduces the probability of contamination.

The launch took place on 12th August 2021 at 21:18 UTC from the European Space and Sounding Rocket Range (Esrangle) in Kiruna, Sweden located 68° N, 21° E at approximately 330 m altitude. Ascent took place over approximately 3:45 hours at an average altitude rate of 4.5 m/s and the balloon reached a maximum altitude of 31.2 km around 23:12 UTC, where it spent approximately 7 min, before descent started. The valve-controlled slow descent was over approximately 3:50 hours with an average vertical speed of -1.5 m/s between 31 and 13 km and an average vertical speed of -8.2 m/s below 13 km after separation of the gondola from the main balloon. Touch-down was at 3:02 UTC. All sampling of air was during the descent to avoid possible contamination of sampled air by the balloon or the gondola itself.

The individual instruments of the payload are listed in Table 1, and Fig. 1 shows the layout of the payload within the gondola structure. The gondola is 2.2 m in height over a base area of 2.6 m x 4 m. In summary, the balloon carried the cryogenic whole air sampler BONBON (Schmidt et al., 1987), five different AirCores (Engel et al., 2017; Wagenhäuser et al., 2021; Laube et al., 2024) and two mid-infrared diode laser spectrometers Pico-SDLA for in-situ measurements of CH<sub>4</sub> and CO<sub>2</sub> (Ghysels et al., 2011, 2014). Position data as well as ambient pressure and temperature were recorded by the Pico-SDLA instrument. In addition, the payload included a newly constructed air sampler for the collection of large air samples in foil bags which was developed based on the lightweight stratospheric air sampler (LISA) (Hooghiem et al., 2018). This sampler will be described in a separate publication and data are not included here The total weight of the payload was approximately 345 kg.

In the post-flight analyses of air samples and AirCores, CO<sub>2</sub> mixing ratios were measured on the WMO X2019 scale (Hall et al., 2021), CH<sub>4</sub> on the WMO X2004A scale (Dlugokencky et al., 2005) and N<sub>2</sub>O on the WMO X2006A (Hall et al., 2007). SF<sub>6</sub> mixing ratios are reported on the WMO X2014 scale (NOAA, 2014).

### 2.2 The Pico-SDLA spectrometer

Pico-SDLA is a balloon-borne spectrometer developed to probe vertical profiles of atmospheric CH<sub>4</sub> and CO<sub>2</sub> (Ghysels et al., 2011, 2014). During the HEMERA-TWIN flight, two Pico-SDLA instruments were launched: Pico-SDLA CH<sub>4</sub> and Pico-STRAT Bi GAZ (H<sub>2</sub>O/CO<sub>2</sub>). The Pico-SDLA CH<sub>4</sub> instrument performed well, whereas Pico-STRAT Bi Gaz measurements suffered from undesired electromagnetic interference for which the source remains undetermined, resulting in spectrum deformations for CO<sub>2</sub>. Therefore, CO<sub>2</sub> measurements are unusable for this flight. Pico-SDLA CH<sub>4</sub> deploys a mid-infrared



**Table 1.** The payload of the HEMERA-TWIN gondola on 12th August 2021. AirCores and air samples were analysed post-flight with Quantum Cascade Laser Spectroscopy (QCLS), Cavity Ring Down Spectroscopy (CRDS) and Gas Chromatography (GC) coupled with an electron capture detector (ECD) or a mass spectrometer (MS), whereas Pico-SDLA is an in-situ instrument measuring in flight.

instrument	analysis
Cryogenic Whole Air Sampler	offline GC-MS, GC-ECD, CRDS
AirCores	offline CRDS, QCLS, sub-sampling for GC-MS
Lightweight stratospheric air sampler LISA	offline QCLS and GC-MS
Pico-SDLA	mid-infrared in-situ spectrometry of CH <sub>4</sub> and CO <sub>2</sub>

distributed-feedback laser emitting at 3.24  $\mu\text{m}$ . The laser beam is propagated in the open atmosphere over a total absorption path length of  $\sim 3.6$  m after multiple reflection. The total weight of the device is approximately 8.5 kg. The simple and robust design of the optical cell minimizes mechanical vibrations, thereby limiting variations of the spectra baseline. Pico-SDLA was integrated into the TWIN gondola in a vertical position. The slow ascent and descent reduced mechanical vibrations, thereby increasing the optical cell instrumental stability.

The wavelength of the laser emission is tuned by ramping the laser driving current every 10 ms. Atmospheric mixing ratios are retrieved from the in situ absorption spectra using a molecular model in conjunction with in-situ atmospheric pressure and temperature measurements. Ambient pressure is measured by an absolute pressure transducer with 0.01 % accuracy (ParoScientific Inc.), measurements are averaged over 0.5 s. Ambient temperature is measured using three fast-response temperature sensors (Sippican) with an uncertainty of 0.2°C and a resolution of 0.1°C on the temperature reading. Measurements are averaged over 1 ms with outliers removed. Sensors are located at each end of the optical cell and at its center. The sensors are known to be susceptible to solar and infrared radiation, but no correction was necessary as measurements took place during night. The temperature uncertainty was improved by an inter-comparison program (Oakley et al., 2011).

The noise of one spectrum is about  $4 \cdot 10^{-4}$  in absorption units. Using single spectra, the measurement precision scales from 48 ppb at ground, down to 15 ppb around the tropopause. For a 1 s averaging time, the precision varies from 25 ppb in the troposphere down to 6 ppb in the UTLS (cf. Table 2). Spectroscopic laboratory work has been conducted in order to determine the appropriate molecular model, accounting for temperature-related effects (Ghysels et al., 2014). This improved the measurement accuracy. The uncertainty budget includes the uncertainty due to the frequency axis and baseline interpolation, the uncertainty due to experimental noise and spectroscopy as well as the uncertainties of pressure and temperature. Table 2 lists the measurement uncertainties of Pico-SDLA CH<sub>4</sub> per levels from the ground up to the balloon ceiling.

### 2.3 Vertical profile measurements with AirCore

The TWIN gondola payload carried three different AirCore packages, from Goethe University Frankfurt (GUF), University of Groningen (Rijksuniversiteit Groningen, RUG) and from Forschungszentrum Jülich (FZJ). The AirCore sampling system is based on a concept first presented by Karion et al. (2010) from an idea originally developed and patented by Tans (2009).



**Table 2.** Uncertainties of Pico-SDLA CH<sub>4</sub> measurements obtained in-flight as a function of pressure level.

pressure range [hPa]	single spectrum precision		1 s precision	
	[ppb]	[%]	[ppb]	[%]
< 50	20	8.7	9	8.6
50–100	20	3.3	9	3.4
100–250	15	2.9	6	2.9
250–60	57	1.7	25	2.1
> 600	48	2.6	20	1.4

AirCores consist of long and narrow stainless steel tubing which at launch time is closed at one end and open at the other. Prior to launch the AirCore is filled with a gas of well-known composition. It evacuates due to decreasing ambient pressure during ascent and reversely samples ambient air with increasing pressure during descent. To avoid loss of sample air or contamination, AirCores may be equipped with a mechanism to automatically close the tube upon landing. After recovery, the sample is analysed for trace gas mole fractions with a continuous-flow gas analyser, and the resulting measurements are attributed to the sampling altitudes. Altitude attribution was based on pressure readings from the Pico-SDLA instrument for both the GUF and RUG AirCores. To attribute the measured trace gas mixing ratios to sampling altitude, the pressure- and temperature-dependent amount of sampled air is calculated as a function of altitude and related to the amount of sample air measured at a constant flow as a function of measurement time. A small amount of fill gas remains in the AirCore tube, that during descent is pushed towards the closed end of the AirCore. During analysis, which is performed in the reverse direction, the remaining fill gas marks the start of the AirCore sample in the measurement time series. In this procedure an easily distinguishable fill gas facilitates the analysis.

Including electronics, AirCores from Frankfurt and Groningen each add only 3 kg to the payload which in a single instrument package makes them deployable with small weather balloons. Deploying them as part of a large instrument package allows the comparison of different configurations. Another larger AirCore, developed and operated by FZJ, was sub-sampled for laboratory GC-MS analysis of halogenated tracers (Laube et al., 2020). Results thereof will be discussed jointly with the GC-MS results from the cryogenic whole air sampler in a companion paper (Laube et al., 2024).

For GUF, the main scientific objective of AirCore measurements is the determination of the mean age of air from CO<sub>2</sub>. Therefore, the AirCores are geometrically designed such that the highest vertical resolution is obtained for the stratosphere (Membrive et al., 2017). They are composed of three different sections with smaller diameters towards the stratospheric end to reduce mixing due to diffusion during the time between sampling and measurement (inner diameters: 7.6, 3.6, 1.76 mm; outer diameters: 8, 4, 2 mm; length: 20, 40, 40 m). Further details have been described by Engel et al. (2017) and Wagenhäuser et al. (2021). The AirCores are constructed from custom-made stainless steel tubing which has been silanised, as suggested by Karion et al. (2010), using Silconert2000® to reduce wall effects and to enhance sample stability during storage. Both AirCores were equipped with Mg(ClO<sub>4</sub>)<sub>2</sub> dryers at the inlet and were automatically closed upon landing.





For the 2021 TWIN gondola launch, one GUF AirCore was equipped with a CO spiking experiment as described by Wagenhäuser et al. (2021) to test the altitude attribution. Because the spiking experiment failed, results of only the AirCore with default configuration are presented here. The initial fill gas had CH<sub>4</sub> and CO<sub>2</sub> mixing ratios close to those expected in the middle stratosphere but was spiked with CO, resulting in a CO mixing ratio of 1436.41 ppb. Mixing with the remaining fill gas is taken into account during the retrieval as described by Wagenhäuser et al. (2021). Thus, the uppermost part of the AirCore profile can be used for scientific evaluation as well.

Starting ~3 hours after landing, GUF AirCores were analysed for CO, CH<sub>4</sub> and CO<sub>2</sub> using a Picarro G2401 cavity ring-down spectrometer (CRDS) and results are reported as dry mixing ratios. The measurement data are calibrated in two steps. First, the raw data was processed with instrument specific parameters that are valid over the long term. Therefore, a linear calibration curve for each component using analyser-specific slope and offset values was applied. These device characteristics were determined in laboratory experiments prior to the campaign. Secondly, the values were corrected for instrumental drift with a day-specific offset determined by measuring a calibration gas tank immediately after the AirCore analysis.

Altitude attribution was performed as described by Engel et al. (2017) and Wagenhäuser et al. (2021). The start and end points of the AirCore sample in the measurement time series were determined using the known mixing ratios of the remaining fill gas that the AirCore tube is filled with prior to the launch and the push gas that is used to push the sample air towards the Picarro instrument during the post-flight analysis. The vertical resolution of the GUF AirCores ranges from about 1000 m at 25 km to better than 300 m around the tropopause and in the troposphere. However, the geometry of the AirCore plays a central role in this uncertainty, so the three individual sections of the GUF AirCore with their different internal diameters and lengths must be taken into account. Further details of the AirCore data analysis including the altitude attribution and fill gas correction were reported by (Wagenhäuser et al., 2021).

The RUG AirCores are similarly designed with smaller diameters towards the stratospheric end to reduce mixing during sampling and sample recovery, each consisting of two sections of different diameters: outer diameter 3/16" and 1/8" with wall thickness ~0.01" and ~0.005", lengths: 37 m and 39 m for one AirCore, 36 m and 38 m for the other. The sections were connected with an externally glued union. One AirCore's inlet was equipped with a Mg(ClO<sub>4</sub>)<sub>2</sub> dryer, while the other AirCore's inlet was left open, to investigate possible water effects on the retrieved profiles. After landing and retrieval, both AirCores were measured on a dual-laser Aerodyne QCLS, detailed below in subsection 2.5 and in Vinković et al. (2022); Tong et al. (2023). The altitude attribution was realized following the approach described in Membrive et al. (2017).

Unfortunately, in both AirCores, the glue connector caused a contamination issue for CO<sub>2</sub> between 11-14 km of altitude. The affected data in this range are not reported, and visible as gaps in the profiles. Upon landing, the closing mechanism of both RUG AirCores malfunctioned, likely due to prolonged cold soak during the flight. The closing attempt drained the batteries, shutting down the data loggers and no temperatures were recorded. Warming of the open-ended tubing between landing (03:02 UTC; T ~-45°C) and capping by the recovery team (approximately 04:15 UTC; T unknown) will have led to a loss of sample from the RUG AirCores, which in consequence will have led to a too-low altitude attribution of the profile. The exact loss and attribution bias cannot be stated with certainty as no temperature data for a volumetric correction were recorded. Indicatively,



180 heating by 10°C would lead to a low bias in altitude attribution of ~300 m in the lower troposphere while the stratospheric part of the profile would be less affected.

Additional uncertainty exists for the stratospheric measurements and altitude attribution: the top and bottom of the retrieved profiles are biased by mixing with the remaining fill gas and the gas employed to push the AirCore air in the instrument. Given uncertainties regarding the gas composition and the actual mixing fractions of the profiles and fill/push gases over the analysis  
185 time, the upper part of the RUG profiles is not reported.

## 2.4 Cryogenic whole air sampling

The cryogenic whole air sampler holds 15 stainless steel sample flasks with volumes 0.58 L (five flasks) or 0.31 L (10 flasks) which were evacuated before the launch. Each flask has an individual inlet system which is opened and closed interactively through telemetry commands from ground. Inlet lines open towards the bottom of the sampler to avoid contact of the sampled  
190 air with any equipment. During sampling, ambient air is cryogenically trapped with liquid neon. The air sampler contains a 10 L reservoir of liquid neon which is filled prior to launch. Further details of the sampler were described by Schmidt et al. (1987). During the HEMERA 2021 launch, the five larger sample flasks were equipped with cotton filters to scrub ozone for accurate measurements of carbonyl sulfide (COS) replacing manganese dioxide on glass wool previously used for this purpose (Andreae et al., 1985; Hofmann et al., 1992; Persson and Leck, 1994; Engel and Schmidt, 1994).

195 In total, 14 samples were successfully collected during descent at altitudes ranging from 30.8 km up to 13.5 km, final sample pressures ranged from 8 bar to 33 bar, corresponding to a total sample volume of 4.6–19.1 L STP. Different types of post-flight analyses of the sampled air were performed at laboratories at Universities Frankfurt, Groningen, Utrecht and at Forschungszentrum Jülich.

## 2.5 Air sample analysis

200 At Frankfurt University, all flask samples were analysed for halogenated compounds with a gas chromatography/mass spectrometry (GC-MS) set-up almost identical to the one described by Hoker et al. (2015) and Schuck et al. (2018), but deploying a quadrupole mass spectrometer in selected ion monitoring mode only. In addition, the air samples were analysed with a semi-continuous gas chromatography/electron capture detection (GC-ECD) set-up for CFC-12 and SF<sub>6</sub> (Engel et al., 2006; Jesswein et al., 2021; Wagenhäuser et al., 2023) and by high resolution cavity ring-down spectroscopy deploying the instrument described in section 2.3 for analysis of CO<sub>2</sub>, CH<sub>4</sub> and CO. Because CO is known to grow in the stainless steel canisters (Novelli et al., 1992), only CO<sub>2</sub> and CH<sub>4</sub> data are presented. SF<sub>6</sub> data from the GC-ECD instrument are measured on the SIO-05 scale, and a conversion factor of 1.0049±0.002 was applied to convert to the WMO X2014 scale (Prinn et al., 2018). One sample, collected without cotton scrubber at 19.3 km altitude, was excluded from further analysis for CO<sub>2</sub> and CH<sub>4</sub> due to an unrealistically high mixing ratio of COS above 5 ppb as detected during GC-MS analysis and a CO<sub>2</sub> mixing ratio above 420 ppm. These  
205 high values might indicate a stability issue during storage. Mixing ratios of SF<sub>6</sub> and N<sub>2</sub>O are shown, as these compounds are chemically inert and unlikely to be affected by storage effects. Furthermore, a sample equipped with cotton scrubber collected at 17.9 km altitude was excluded because unrealistically high mixing ratios of several trace gases were measured, including  
210





**Table 3.** Instrumental precision and average error of flask analysis.

	CRDS	QCLS	GC-ECD	GC-MS
CO <sub>2</sub>	0.01 % (0.025 ppm)	0.05 % (0.2 ppm)	–	–
CH <sub>4</sub>	0.05 % (0.2 ppb)	0.03 % (0.6 ppb)	–	–
SF <sub>6</sub>	–	–	0.6 % (0.05 ppt)	0.6 % (0.06 ppt)
N <sub>2</sub> O	–	0.03 % (0.12 ppb)	–	–

CO<sub>2</sub>, SF<sub>6</sub> and several halogenated compounds, which points to a contamination of this sample. All measurements of halo-  
 genated tracers with the GC-MS setup from the cryogenic air samples will be presented in a companion paper (Laube et al.,  
 215 2024).

At RUG, in September of 2021, the cryosamples were analysed on a quantum cascade laser spectrometer (QCLS; model  
 TILDAS Dual, Aerodyne Research Inc., MA, USA). Its first laser (scan centered around wavenumber 1275.5) observes CH<sub>4</sub>,  
 N<sub>2</sub>O and H<sub>2</sub>O, while its second laser (around wavenumber 2050.6) observes COS, CO<sub>2</sub> and CO. The cavity of the analyser  
 is maintained at a pressure of  $50 \pm 0.002$  Torr ( $\sim 66$  hPa) and a temperature of  $250 \pm 0.002^\circ\text{C}$ . Under these conditions the  
 220 equivalent volume of the optical cavity is  $\sim 10$  cm<sup>3</sup> (geometric volume  $\sim 150$  cm<sup>3</sup>), and a precision better than 0.6 ppb, 0.12 ppb,  
 and 0.20 ppm is attained for CH<sub>4</sub>, N<sub>2</sub>O and CO<sub>2</sub>, respectively ( $1\sigma$  of individual samples, collected at 1 Hz). Sample flowrate is  
 $\sim 50$  sccm.

Measurements are calibrated against multiple compressed air working standards (prepared in-house). Each working standard  
 was measured repeatedly before, during and after the samples to control for conceivable drift. QCLS response functions were  
 225 obtained by linearly fitting the measurements of the standards to their assigned values, after linearly interpolating these mea-  
 surements in time. The obtained time-dependent response functions were applied to raw measurements, and the curve fitting  
 procedure is repeated to obtain the final sample results. Running in tightly controlled laboratory conditions, the performance  
 of the QCLS was excellent and the uncertainties in our final values are dominated by the inaccuracies in the assigned values of  
 our working standards (i.e., not instrumental noise or drift), taken to be  $\pm 1$  ppb,  $\pm 0.3$  ppb,  $\pm 0.10$  ppm, respectively for CH<sub>4</sub>,  
 230 N<sub>2</sub>O and CO<sub>2</sub>. We note, however, that this assessment may not hold true for stratospheric samples, of which the mixing ratios  
 of multiple trace gas species are significantly lower. For these samples, unknown (but unexpected) non-linearities of the QCLS  
 response may reduce the attained accuracy. Such conceivable but unlikely bias cannot be compensated for due to absence of  
 suitable calibration gases and data were evaluated assuming a linear response of the instrument.

The analytical procedure at Forschungszentrum Jülich consists of three main steps: 1) cryogenic extraction and pre-concen-  
 235 tration of trace gases at  $\sim -78^\circ\text{C}$ , immediately followed by thermal desorption at  $\sim 95^\circ\text{C}$ , 2) separation by gas chromatography  
 (Agilent 6890 GC with a 60 m GS GasPro column and a temperature program from  $-10$  to  $200^\circ\text{C}$ ), and 3) detection with a  
 triple-sector mass spectrometer (Waters AutoSpec MS) in selected ion monitoring mode. Further details are described in the  
 companion paper by Laube et al. (2024). SF<sub>6</sub> mixing ratios are reported on the WMO X2014 scale with an average precision  
 of 0.6 % (0.06 ppt).



240 Precision values for the analysis of AirCores and cryo sampled flasks are summarized in Table 3. All instruments meet the minimum requirements to ensure that data are useful as defined for the World Meteorological Organisation Global Climate Observing System programme (WMO, 2024). These are 0.5 ppm for CO<sub>2</sub>, 5 ppb for CH<sub>4</sub> and 0.3 ppb for N<sub>2</sub>O. As ideal requirements, beyond which no further improvement seems necessary, 0.1 ppm, 1 ppb and 0.05 ppb are defined for these three gases. This ideal data quality goal is met for CO<sub>2</sub> by the CRDS instrument and the QCL instrument comes close. WMO does  
245 not define a data quality target for SF<sub>6</sub>.

## 2.6 Age of air calculations

Mean age of air values were derived from SF<sub>6</sub> measurements and independently from simultaneous CO<sub>2</sub> and CH<sub>4</sub> measurements following the procedure described by Garny et al. (2024b) using the *AoA\_from\_convolution* python package version 1.0.0 (Wagenhäuser et al., 2024). The package uses the NOAA Greenhouse Gas Marine Boundary Layer Reference for SF<sub>6</sub>,  
250 CO<sub>2</sub> and CH<sub>4</sub> trace gas mixing ratio reference time series at the tropical surface ± 17.5° around the equator (Garny et al., 2024c). Mean age values below 1 year are omitted due to numerical reasons of the software implementation. Regarding SF<sub>6</sub>, these mean age calculations do not account for the mesospheric sink, which leads to apparently older SF<sub>6</sub> mean ages (Leedham Elvidge et al., 2018; Garny et al., 2024a). For CO<sub>2</sub>, the software first uses CH<sub>4</sub> mixing ratios to account for stratospheric CO<sub>2</sub> production from CH<sub>4</sub> degradation. This corrected CO<sub>2</sub> mixing ratio is then used to derive the mean age. Note that there  
255 is no correction implemented for the upward propagation of the seasonal cycle of CO<sub>2</sub> in the software. Therefore, mean age values below 2 years derived from CO<sub>2</sub> measurements are problematic (Garny et al., 2024a).

## 3 Comparison of trace gas mixing ratio and age of air profiles

Figures 2, 3 and 4 show the vertical profiles of CH<sub>4</sub>, CO<sub>2</sub> and N<sub>2</sub>O, respectively. For CH<sub>4</sub>, also data from the Pico-SDLA instrument are included. It is the only instrument that also provides data for the balloon ascent. For CO<sub>2</sub> and N<sub>2</sub>O, only data  
260 from AirCores and the cryo samples are shown. Left hand panels show the vertical profile of absolute mixing ratios, right hand panels show mixing ratios relative to results from the analysis of air samples at University of Frankfurt, except for N<sub>2</sub>O which was not measured at this laboratory. High resolution measurements have been averaged over the sampling period of each individual sample. The error bars in the right hand panels indicate the variability of the high resolution data over the sample collection time.

265 In the troposphere, CO<sub>2</sub> mixing ratios show variability between 403 ppm and 413 ppm, and CH<sub>4</sub> mixing ratios vary between 1920 ppb and 1980 ppb in the two AirCore datasets. The high resolution Pico data exhibits a tropospheric mixing ratio range from 1920 ppb to 2100 ppb. Above 10 km, CH<sub>4</sub> mixing ratios decrease slowly up to 17 km and decrease steeper with altitude above. Above 20 km, several layers of low CH<sub>4</sub> mixing ratios are apparent in the Pico data which cannot be resolved by the other measurement methods. CO<sub>2</sub>, in contrast, starts to increase at an altitude of approximately 7 km and starts to decrease at  
270 around 14 km altitude. A minimum is reached around 24 km altitude. Comparing results from analysis of AirCore and flask samples, N<sub>2</sub>O behaves similar to CH<sub>4</sub>.

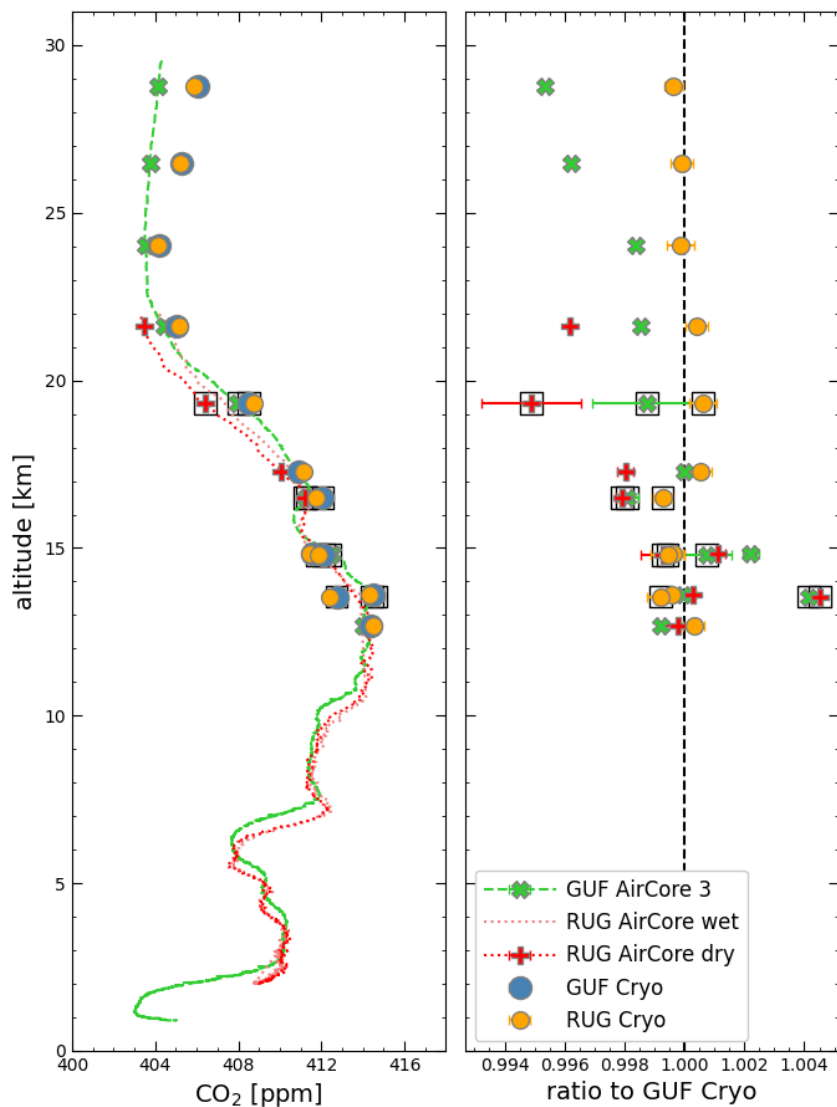


**Figure 2.** Vertical profiles of CO<sub>2</sub> (left) and comparison with results from the cryo samples as measured at University of Frankfurt (right). To compare results of the high resolution observations with the samples, the mean value over the sampling period has been calculated using the standard deviation as error bars. Error bars may be smaller than symbol size. Mixing ratios of samples with the cotton scrubber are highlighted by the square symbol.

Comparing the two AirCore systems (i. e., GUF and RUG), for which data analysis and altitude attribution is done independently, there is an offset of approximately 300 m with the Groningen AirCores being attributed systematically to lower altitudes. As described above, this may be caused by the uncorrected loss of sample after landing when the automatic closing

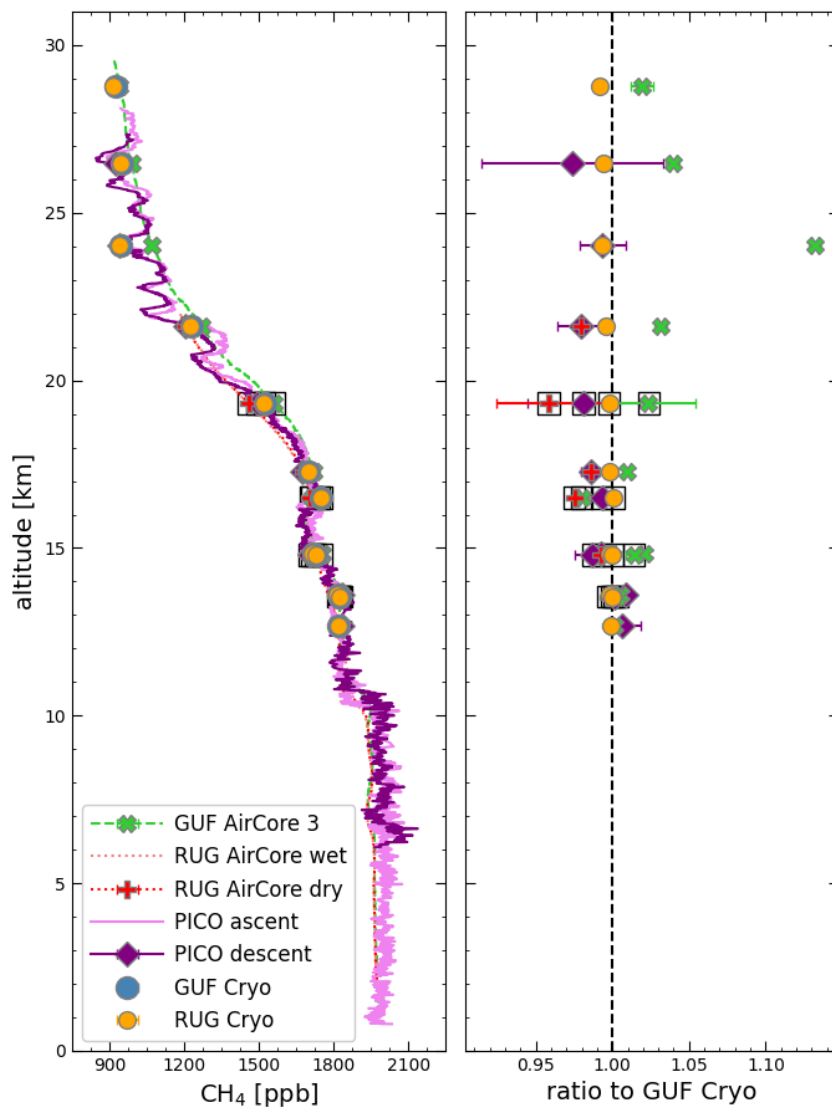


**Figure 3.** As Fig. 2, for CH<sub>4</sub>

275 of the AirCores failed. Comparing the two profiles retrieved from the RUG AirCores with and without drying on sampling, the water vapour did not cause a major bias in the retrieved CO<sub>2</sub> and CH<sub>4</sub> molar fractions. In fact, the biggest differences were found in the stratospheric part of the profile, where the atmospheric H<sub>2</sub>O content is negligible. In the troposphere, differences between the two AirCores at comparable altitudes reached up to 0.4 ppm and 2 ppb for CO<sub>2</sub> and CH<sub>4</sub>, respectively. However, the stratospheric part of the profiles showed differences up to 1.3 ppm for CO<sub>2</sub> and 5 ppb for CH<sub>4</sub>. The reasons behind these

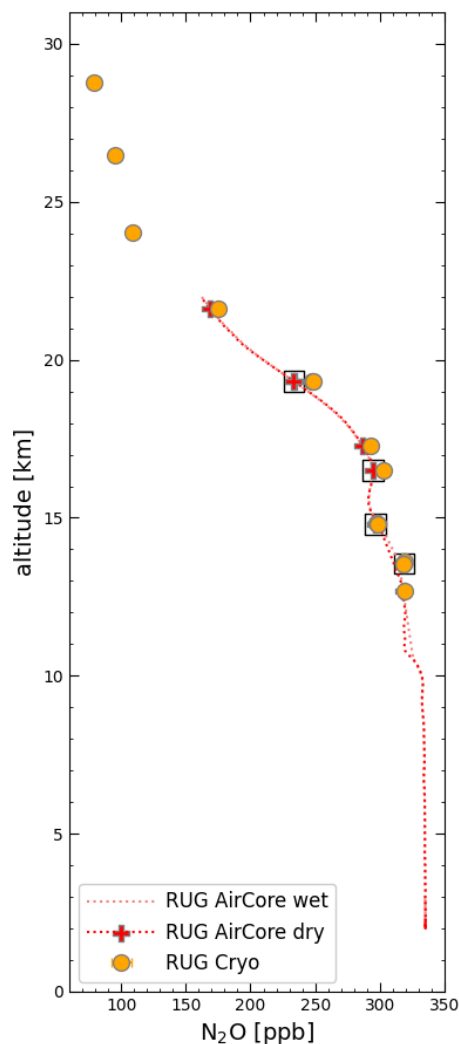


**Figure 4.** As Fig. 2, for N<sub>2</sub>O. N<sub>2</sub>O was only measured at University of Groningen and no inter-laboratory comparison is possible.

280 differences remained overall unclear, but we speculate they could be ascribed to some remaining mixing with the AirCores' fill gases, or to the interaction of the Mg(ClO<sub>4</sub>)<sub>2</sub> dryer with other gas species in the stratosphere.

All flask samples were analysed post-flight at Universities of Frankfurt and Groningen with the identical instruments that were used for post-flight analyses of AirCores. For both laboratories, good agreement within the respective instrumental precisions is found. For CO<sub>2</sub>, the average difference is 0.14 ppm, varying between 0.04 ppm and 0.22 ppm, for CH<sub>4</sub> it is 4.3 ppb, 285 varying between 1.8 ppb and 7.4 ppb. Because of the good agreement between the two datasets, in the following, measurement results obtained from the cryo sampler at University of Frankfurt are used as reference for comparison except for N<sub>2</sub>O, which



was only measured at University of Groningen. Around 14.8 km and 13.5 km altitude overlapping samples with and without a scrubber were collected, although for technical reasons not covering the exact same altitude range, as only one sample flask could be opened or closed at a time. Mixing ratios of CO<sub>2</sub>, CH<sub>4</sub> and N<sub>2</sub>O agree well for those two sample pairs.

290 The Pico-SDLA is the only instrument of the payload that provides data for the balloon ascent. Although for the lowest altitude part of the profiles the time difference between ascent and descent is almost 7 hours, the two measurements agree closely. The spectrometer can resolve small structures in the stratosphere much better than the AirCores which provide a smoothed profile in comparison to Pico-SDLA. When averaging over sample collection times of the cryo sampler, very good agreement is found with CH<sub>4</sub> mixing ratios measured post-flight in the laboratories at Universities of Frankfurt and Groningen.

295 Also, for the sample collected at 24 km altitude, when the spectrometer recorded a local minimum of CH<sub>4</sub> mixing ratios which is not captured by the AirCore observations, both independent post-flight analyses agree. On the right hand side of Fig. 2 and 3, the variability of the Pico data is reflected by the larger error bars of the integrated Pico data, most pronounced for the air sample collected at 26.6 km. On average, integrated Pico data deviate from the sample analysis results in Frankfurt by 9 ppb, with a minimum deviation of 6 ppb and a maximum difference of 25 ppb. In the troposphere, Pico data are noisier than

300 in the stratosphere, and they are slightly offset towards higher mixing ratios compared to the AirCore profiles. Mixing ratios follow those derived from AirCore measurements, but with more fine structure, as the Pico-SDLA directly records in situ data, whereas AirCores are a technique with an inherent averaging kernel. Above 20 km, the Pico profile reveals several layers of lower CH<sub>4</sub> mixing ratios, which cannot be resolved by air samples nor the AirCores.

AirCore data have also been averaged over the sampling interval of each cryo sampler flask. Differences relative to the direct

305 measurement of CO<sub>2</sub> and CH<sub>4</sub> might partly arise from the uncertainty in altitude attribution. In addition, AirCores do provide a continuously sampled profile, but due to molecular diffusion some averaging and smoothing with altitude occurs. This becomes most evident comparing the CH<sub>4</sub> profile derived from AirCore measurements to the in situ recording of CH<sub>4</sub> mixing ratios from the Pico spectrometer. The Pico recorded several fine structures above 20 km altitude which are not apparent in the AirCore profiles. Compared to the cryo sampler analyses at University of Frankfurt, GUF AirCore CH<sub>4</sub> integrals tend to be higher by

310 on average 35 ppb, with a minimum difference of 2.2 ppb and the maximum difference of 125.0 ppb, which is observed for the sample collected during a CH<sub>4</sub> minimum of the Pico profile.

In CO<sub>2</sub>, AirCore profiles tend to be at lower mixing ratios in comparison to the cryo sampler analyses, in particular at higher altitudes. For data from University of Frankfurt, the maximum deviation is 1.55 ppm, best agreement found is within 0.14 ppm. Similar results are obtained for the AirCores from University of Groningen for CO<sub>2</sub> and N<sub>2</sub>O.

315 Figure 5 compares the results of SF<sub>6</sub> measurements from the air samples in two different laboratories, at University of Frankfurt and at Forschungszentrum Jülich. In Frankfurt, SF<sub>6</sub> is measured with GC-ECD, in Jülich with GC-MS. Similar to CO<sub>2</sub>, SF<sub>6</sub> mixing ratios decrease above the tropopause with the steepest vertical gradient occurring between 17 and 24 km. Results of the two independent measurements agree within their respective uncertainty with a mean difference of 0.04 ppt, varying from 0.01 ppt to 0.27 ppt, corresponding to a relative difference range 0.08 % to 2.7 %. For each instrument, results for

320 the overlapping samples with and without the ozone scrubber agree within the uncertainty. As for CO<sub>2</sub> and CH<sub>4</sub>, the steepest



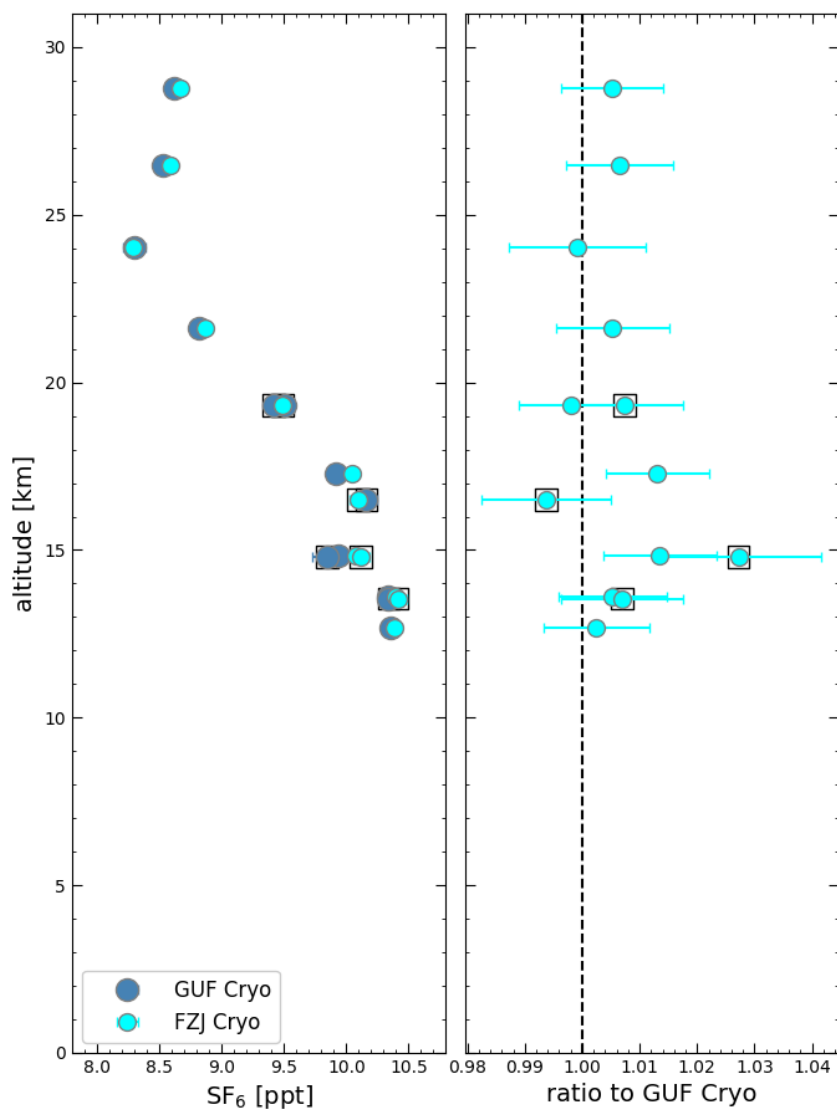


**Figure 5.** Vertical profiles of SF<sub>6</sub> analysed from air samples with GC-ECD (GUF) and GC-MS (FZJ). Error bars of absolute values (left) are smaller than symbol size.

gradient in the SF<sub>6</sub> mixing ratios occurs between 17 and 24 km altitude and, as shown in Fig. 6, there is a clear correlation between SF<sub>6</sub> and the two other greenhouse gases.

Figure 7 compares values for the age of air derived according to Garny et al. (2024b) from mixing ratios of CO<sub>2</sub> and SF<sub>6</sub> with the tropical marine boundary layer mixing ratios as reference time series (Wagenhäuser et al., 2024). Comparing the results from the flask samples to the AirCore analysis exemplary for the GUF AirCore, the systematically higher CO<sub>2</sub> mixing ratios

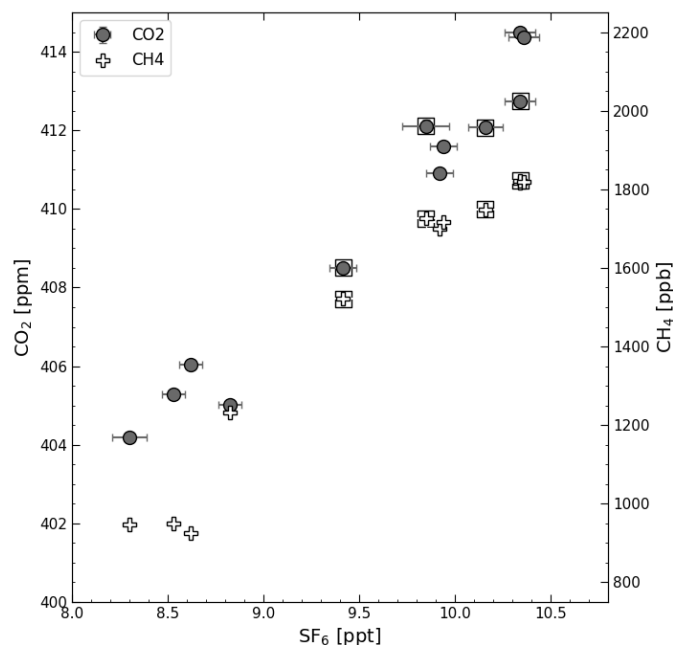


**Figure 6.** Correlation of CO<sub>2</sub> and CH<sub>4</sub> with SF<sub>6</sub> as analysed from air samples. Mixing ratios of samples with the cotton scrubber are highlighted by the square symbol.

obtained from the flask samples at the highest altitudes are reflected as lower age of air values. However, the general structure of the profiles agree, in particular at altitudes below 20 km. This confirms that AirCores are a measurement technique suited to derive age of air profiles from CO<sub>2</sub> observations.

For CO<sub>2</sub>, systematically lower ages are derived, with the difference increasing with altitude. This agrees with findings by Ray et al. (2024), who consistently analysed a large number of dataset from aircraft and balloon borne measurements for the periods 1994–2000 and 2021–2024, including AirCore data for the latter period. In the 2021 HEMERA TWIN dataset, the difference increases to 1.5 years at altitudes around 24 km and above. Using the bias correction described by Garny et al. (2024a) to account for chemical sinks of SF<sub>6</sub> reduces the SF<sub>6</sub> age by 0.05 years to 1.67 years with an average reduction of 0.55 years. The corrected values range from 1–5 years with maximum ages of 4.4–5.1 years above 20 km altitude. The corrected SF<sub>6</sub> agrees better with the value derived from CO<sub>2</sub> with the average difference reducing from 0.66 years to 0.08 years when applying the correction.

#### 4 Conclusions

Within the HEMERA balloon infrastructure project coordinated by the French space agency CNES, the openly constructed TWIN gondola was launched from Kiruna, Sweden, in August 2021. The gondola was equipped with two different air samplers,

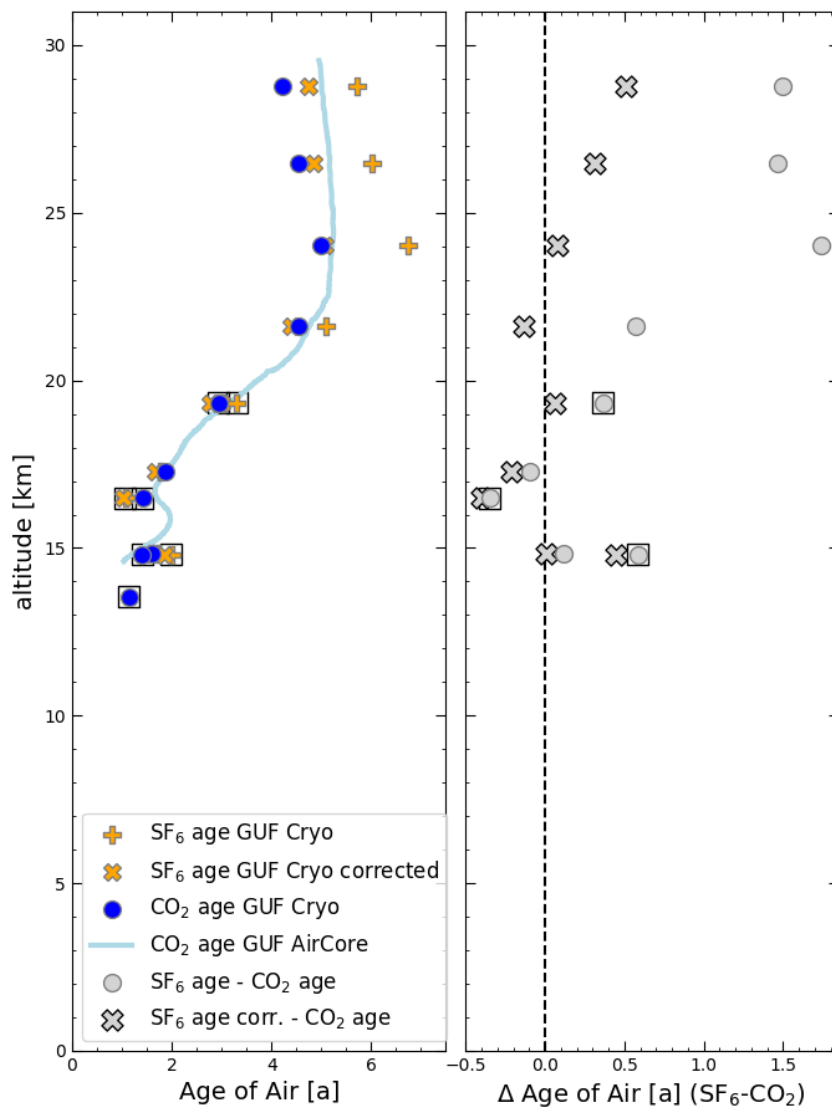


**Figure 7.** Age of air values derived from CO<sub>2</sub> and SF<sub>6</sub> mixing ratios of flask air samples and AirCore CO<sub>2</sub> mixing ratios. Samples with the cotton scrubber are highlighted by the square symbol. “X” markers represent Ae of air values from SF<sub>6</sub> mixing ratios corrected using the method by Garny et al. (2024a).

340 three different types of AirCores and the mid-infrared diode laser spectrometer Pico-SDLA for in-situ measurements of CH<sub>4</sub>. A maximum altitude of 31.2 km was reached. Here, we reported on analysis results for CO<sub>2</sub>, CH<sub>4</sub> and SF<sub>6</sub> from cryogenically collected air samples in stainless steel flasks. Samples were analysed post-flight in different laboratories using optical and



gas chromatography based measurement techniques. Mixing ratios of all three greenhouse gases agree well for the different analyses.

345 Results are compared to vertical profiles of CO<sub>2</sub> and CH<sub>4</sub> derived from AirCores and for CH<sub>4</sub> to the measurements with the Pico-SDLA. The latter instrument records more fine structure at altitudes above 20 km, which is not apparent in the AirCore data with much smoother profiles. While the agreement between the Pico measurements and the air sample analysis is very good for CH<sub>4</sub>, AirCore derived CH<sub>4</sub> deviates, likely because the AirCore cannot resolve the observed minima in the CH<sub>4</sub> profile. Additional uncertainty arises from the altitude attribution of the AirCore profiles. This becomes more apparent in the case of  
350 CO<sub>2</sub>, for which the difference between air sample analyses and Aircore profiles seem to increase with altitude. In addition, differences between two independent AirCore datasets are observed, with altitude differences of individual features of up to 300 m.

For CO<sub>2</sub> and SF<sub>6</sub> age of air was derived from the observations following the approach by Garny et al. (2024b). At altitudes of 24 km and above, maximum ages between 5.8 and 6.5 years were obtained from SF<sub>6</sub> mixing ratios which reduced to 4.4–  
355 5.1 years after correction of the chemical sink according to Garny et al. (2024a). Age of air values derived from CO<sub>2</sub> are systematically lower, with the difference increasing with altitude, in agreement with finding from other datasets. Up to an altitude of 25 km age of air derived from AirCore analysis of CO<sub>2</sub> agrees well with flask sample data, at higher altitudes differences occur. Accounting for chemical sinks of SF<sub>6</sub>, the SF<sub>6</sub>-based Age of Air decreases and better agrees with CO<sub>2</sub>-derived age of air within 0.5 years. Recently, Ray et al. (2024) proposed a new technique of deriving age of air from simultaneous measurements  
360 of several long-lived trace gases. The data set presented here, containing CO<sub>2</sub>, CH<sub>4</sub> and SF<sub>6</sub>, should be well suited for this approach. The dataset, which will be complemented by further data of halogenated long-lived trace gases (Laube et al., 2024), will enable further age of air evaluations.

*Data availability.* Observational data are available from <https://zenodo.org/records/13918431> (Schuck et al., 2024).

*Author contributions.* AE, AZ, GD, JL, MEP, NA, SLB, SvH, TJS, TK and TW operated the instrumentation in the field and contributed  
365 to data analysis, CvdV contributed to the campaign preparation and laboratory work. AZ, JL, SvH, SLB, MEP, TJS and TW performed post-flight sample analysis. JD and KM performed further data analysis of GUF AirCore data. TJS drafted the manuscript. All coauthors contributed to the scientific discussion and improvements of the manuscript.

*Competing interests.* At least one of the (co-)authors is a member of the editorial board of Atmospheric Chemistry and Physics.

*Acknowledgements.* We are grateful for the support from the technical staff before, during, and after the campaign, especially from Anne  
370 Richter, Andreas Sitnikov, Jochen Barthel, and Vicheith Tan (FZJ) and Laurin Merkel GUF). We acknowledge the support from local staff at

<https://doi.org/10.5194/egusphere-2024-3279>

Preprint. Discussion started: 25 October 2024

© Author(s) 2024. CC BY 4.0 License.



ESRANGE and from the CNES team. We acknowledge NOAA Global Monitoring Laboratory for providing surface measurements of CO<sub>2</sub> and SF<sub>6</sub> for derivation of age of air.

*Financial support.* This research has been supported by the DFG collaborative research program “The Tropopause Region in a Changing Atmosphere” TRR 301 – Project-ID 428312742. and by the European Research Council (grant no. EXC3ITE (678904) and COS-OCS 375 (742798) and HEMERA (730790)).



## References

- Abalos, M., Calvo, N., Benito-Barca, S., Garny, H., Hardiman, S. C., Lin, P., Andrews, M. B., Butchart, N., Garcia, R., Orbe, C., Saint-Martin, D., Watanabe, S., and Yoshida, K.: The Brewer–Dobson circulation in CMIP6, *Atmospheric Chemistry and Physics*, 21, 13 571–13 591, <https://doi.org/10.5194/acp-21-13571-2021>, 2021.
- 380 Andreae, M. O., Ferek, R. J., Bermond, F., Byrd, K. P., Engstrom, R. T., Hardin, S., Houmère, P. D., LeMarrec, F., Raemdonck, H., and Chatfield, R. B.: Dimethyl sulfide in the marine atmosphere, *Journal of Geophysical Research: Atmospheres*, 90, 12 891–12 900, <https://doi.org/https://doi.org/10.1029/JD090iD07p12891>, 1985.
- Andrews, A. E., Boering, K. A., Daube, B. C., Wofsy, S. C., Loewenstein, M., Jost, H., Podolske, J. R., Webster, C. R., Herman, R. L., Scott, D. C., Flesch, G. J., Moyer, E. J., Elkins, J. W., Dutton, G. S., Hurst, D. F., Moore, F. L., Ray, E. A., Romashkin, P. A., and Strahan, S. E.:  
385 Mean ages of stratospheric air derived from in situ observations of CO<sub>2</sub>, CH<sub>4</sub>, and N<sub>2</sub>O, *Journal of Geophysical Research: Atmospheres*, 106, 32 295–32 314, <https://doi.org/https://doi.org/10.1029/2001JD000465>, 2001.
- Austin, J. and Li, F.: On the relationship between the strength of the Brewer–Dobson circulation and the age of stratospheric air, *Geophysical Research Letters*, 33, <https://doi.org/10.1029/2006GL026867>, 2006.
- Bönisch, H., Engel, A., Curtius, J., Birner, T., and Hoor, P.: Quantifying transport into the lowermost stratosphere using simultaneous in-situ  
390 measurements of SF<sub>6</sub> and CO<sub>2</sub>, *Atmospheric Chemistry and Physics*, 9, 5905–5919, <https://doi.org/10.5194/acp-9-5905-2009>, 2009.
- Brinckmann, S., Engel, A., Bönisch, H., Quack, B., and Atlas, E.: Short-lived brominated hydrocarbons – observations in the source regions and the tropical tropopause layer, *Atmospheric Chemistry and Physics*, 12, 1213–1228, <https://doi.org/10.5194/acp-12-1213-2012>, 2012.
- Diallo, M., Legras, B., Ray, E., Engel, A., and Añel, J. A.: Global distribution of CO<sub>2</sub> in the upper troposphere and stratosphere, *Atmospheric Chemistry and Physics*, 17, 3861–3878, <https://doi.org/10.5194/acp-17-3861-2017>, 2017.
- 395 Dlugokencky, E. J., Myers, R. C., Lang, P. M., Masarie, K. A., Crotwell, A. M., Thoning, K. W., Hall, B. D., Elkins, J. W., and Steele, L. P.: Conversion of NOAA atmospheric dry air CH<sub>4</sub> mole fractions to a gravimetrically prepared standard scale, *Journal of Geophysical Research: Atmospheres*, 110, <https://doi.org/https://doi.org/10.1029/2005JD006035>, 2005.
- Eichinger, R., Dietmüller, S., Garny, H., Šácha, P., Birner, T., Bönisch, H., Pitari, G., Visoni, D., Stenke, A., Rozanov, E., Revell, L., Plummer, D. A., Jöckel, P., Oman, L., Deushi, M., Kinnison, D. E., Garcia, R., Morgenstern, O., Zeng, G., Stone, K. A., and Schofield,  
400 R.: The influence of mixing on the stratospheric age of air changes in the 21st century, *Atmospheric Chemistry and Physics*, 19, 921–940, <https://doi.org/10.5194/acp-19-921-2019>, 2019.
- Engel, A. and Schmidt, U.: Vertical profile measurements of carbonylsulfide in the stratosphere, *Geophysical Research Letters*, 21, 2219–2222, <https://doi.org/https://doi.org/10.1029/94GL01461>, 1994.
- Engel, A., Strunk, M., Müller, M., Haase, H.-P., Poss, C., Levin, I., and Schmidt, U.: Temporal development of total chlorine in the high-  
405 latitude stratosphere based on reference distributions of mean age derived from CO<sub>2</sub> and SF<sub>6</sub>, *Journal of Geophysical Research: Atmospheres*, 107, ACH 1–1–ACH 1–11, <https://doi.org/https://doi.org/10.1029/2001JD000584>, 2002.
- Engel, A., Bönisch, H., Brunner, D., Fischer, H., Franke, H., Günther, G., Gurk, C., Hegglin, M., Hoor, P., Königstedt, R., Krebsbach, M., Maser, R., Parchatka, U., Peter, T., Schell, D., Schiller, C., Schmidt, U., Spelten, N., Szabo, T., Weers, U., Wernli, H., Wetter, T., and Wirth, V.: Highly resolved observations of trace gases in the lowermost stratosphere and upper troposphere from the Spurt project: an  
410 overview, *Atmospheric Chemistry and Physics*, 6, 283–301, <https://doi.org/10.5194/acp-6-283-2006>, 2006.





- Engel, A., Möbius, T., Bönisch, H., Schmidt, U., Heinz, R., Levin, I., Atlas, E., Aoki, S., Nakazawa, T., Sugawara, S., Moore, F., Hurst, D., Elkins, J., Schauffler, S., Andrews, A., and Boering, K.: Age of stratospheric air unchanged within uncertainties over the past 30 years, *Nature Geoscience*, 2, 28–31, <https://doi.org/10.1038/ngeo388>, 2009.
- Engel, A., Bönisch, H., Ullrich, M., Sitals, R., Membrive, O., Danis, F., and Crevoisier, C.: Mean age of stratospheric air derived from  
415 AirCore observations, *Atmospheric Chemistry and Physics*, 17, 6825–6838, <https://doi.org/10.5194/acp-17-6825-2017>, 2017.
- Garny, H., Eichinger, R., Laube, J. C., Ray, E. A., Stiller, G. P., Bönisch, H., Saunders, L., and Linz, M.: Correction of stratospheric age of air (AoA) derived from sulfur hexafluoride (SF<sub>6</sub>) for the effect of chemical sinks, *Atmospheric Chemistry and Physics*, 24, 4193–4215, <https://doi.org/10.5194/acp-24-4193-2024>, 2024a.
- Garny, H., Ploeger, F., Abalos, M., Bönisch, H., Castillo, A., von Clarmann, T., Diallo, M., Engel, A., Laube, J. C., Linz, M., Neu, J.,  
420 Podglajen, A., Ray, E., Rivoire, L., Saunders, L. N., Stiller, G., Voet, F., Wagenhäuser, T., and Walker, K. A.: Age of stratospheric air: Progress on processes, observations and long-term trends, accepted for publication in *Review of Geophysics*, 2024b.
- Garny, H., Saunders, L., Voet, F., Ray, E., von Clarmann, T., Bönisch, H., Engel, A., Laube, J., Linz, M., Stiller, G., Wagenhäuser, T., and Walker, K. A.: Age of stratospheric air: observational data sets, <https://doi.org/10.5281/zenodo.11267157>, 2024c.
- Ghysels, M., Gomez, L., Cousin, J., Amarouche, N., Jost, H., and Durry, G.: Spectroscopy of CH<sub>4</sub> with a difference-frequency generation  
425 laser at 3.3 micron for atmospheric applications, *Applied Physics B*, 104, 989–1000, <https://doi.org/10.1007/s00340-011-4665-2>, 2011.
- Ghysels, M., Gomez, L., Cousin, J., Tran, H., Amarouche, N., Engel, A., Levin, I., and Durry, G.: Temperature dependences of air-broadening, air-narrowing and line-mixing coefficients of the methane  $\nu_3$  R(6) manifold lines—Application to in-situ measurements of atmospheric methane, *Journal of Quantitative Spectroscopy and Radiative Transfer*, 133, 206–216, <https://doi.org/10.1016/j.jqsrt.2013.08.003>, 2014.
- Hall, B. D., Dutton, G. S., and Elkins, J. W.: The NOAA nitrous oxide standard scale for atmospheric observations, *Journal of Geophysical  
430 Research: Atmospheres*, 112, <https://doi.org/https://doi.org/10.1029/2006JD007954>, 2007.
- Hall, B. D., Crotwell, A. M., Kitzis, D. R., Mefford, T., Miller, B. R., Schibig, M. F., and Tans, P. P.: Revision of the World Meteorological Organization Global Atmosphere Watch (WMO/GAW) CO<sub>2</sub> calibration scale, *Atmospheric Measurement Techniques*, 14, 3015–3032, <https://doi.org/10.5194/amt-14-3015-2021>, 2021.
- Hall, T. M. and Plumb, R. A.: Age as a diagnostic of stratospheric transport, *Journal of Geophysical Research: Atmospheres*, 99, 1059–1070,  
435 <https://doi.org/https://doi.org/10.1029/93JD03192>, 1994.
- Hauck, M., Bönisch, H., Hoor, P., Keber, T., Ploeger, F., Schuck, T. J., and Engel, A.: A convolution of observational and model data to estimate age of air spectra in the northern hemispheric lower stratosphere, *Atmospheric Chemistry and Physics*, 20, 8763–8785, <https://doi.org/10.5194/acp-20-8763-2020>, 2020.
- Hofmann, U., Hofmann, R., and Kesselmeier, J.: Cryogenic trapping of reduced sulfur compounds using a nafion drier and cotton wadding  
440 as an oxidant scavenger, *Atmospheric Environment. Part A. General Topics*, 26, 2445–2449, [https://doi.org/https://doi.org/10.1016/0960-1686\(92\)90374-T](https://doi.org/https://doi.org/10.1016/0960-1686(92)90374-T), 1992.
- Hoker, J., Obersteiner, F., Bönisch, H., and Engel, A.: Comparison of GC/time-of-flight MS with GC/quadrupole MS for halocarbon trace gas analysis, *Atmos. Meas. Tech.*, 8, 2195–2206, <https://doi.org/10.5194/amt-8-2195-2015>, 2015.
- Hooghiem, J. J. D., de Vries, M., Been, H. A., Heikkinen, P., Kivi, R., and Chen, H.: LISA: a lightweight stratospheric air sampler, *Atmo-  
445 spheric Measurement Techniques*, 11, 6785–6801, <https://doi.org/10.5194/amt-11-6785-2018>, 2018.
- Jesswein, M., Bozem, H., Lachnitt, H.-C., Hoor, P., Wagenhäuser, T., Keber, T., Schuck, T., and Engel, A.: Comparison of inorganic chlorine in the Antarctic and Arctic lowermost stratosphere by separate late winter aircraft measurements, *Atmospheric Chemistry and Physics*, 21, 17 225–17 241, <https://doi.org/10.5194/acp-21-17225-2021>, 2021.



- Karion, A., Sweeney, C., Tans, P., and Newberger, T.: AirCore: An Innovative Atmospheric Sampling System, *Journal of Atmospheric and Oceanic Technology*, 27, 1839–1853, <https://doi.org/https://doi.org/10.1175/2010JTECHA1448.1>, 2010.
- 450 Kolonjari, F., Sheese, P. E., Walker, K. A., Boone, C. D., Plummer, D. A., Engel, A., Montzka, S. A., Oram, D. E., Schuck, T., Stiller, G. P., and Toon, G. C.: Validation of Atmospheric Chemistry Experiment Fourier Transform Spectrometer (ACE-FTS) chlorodifluoromethane (HCFC-22) in the upper troposphere and lower stratosphere, *Atmospheric Measurement Techniques*, 17, 2429–2449, <https://doi.org/10.5194/amt-17-2429-2024>, 2024.
- 455 Kovács, T., Feng, W., Totterdill, A., Plane, J. M. C., Dhomse, S., Gómez-Martín, J. C., Stiller, G. P., Haenel, F. J., Smith, C., Forster, P. M., García, R. R., Marsh, D. R., and Chipperfield, M. P.: Determination of the atmospheric lifetime and global warming potential of sulfur hexafluoride using a three-dimensional model, *Atmospheric Chemistry and Physics*, 17, 883–898, <https://doi.org/10.5194/acp-17-883-2017>, 2017.
- Krzysztofak, G., Catoire, V., Dudok de Wit, T., Kinnison, D. E., Ravishankara, A. R., Brocchi, V., Atlas, E., Bozem, H., Commane, R., 460 D’Amato, F., Daube, B., Diskin, G. S., Engel, A., Friedl-Vallon, F., Hintsä, E., Hurst, D. F., Hoor, P., Jegou, F., Jucks, K. W., Kleinböhl, A., Küllmann, H., Kort, E. A., McKain, K., Moore, F. L., Obersteiner, F., Ramos, Y. G., Schuck, T., Toon, G. C., Viciani, S., Wetzel, G., Williams, J., and Wofsy, S. C.: N<sub>2</sub>O Temporal Variability from the Middle Troposphere to the Middle Stratosphere Based on Airborne and Balloon-Borne Observations during the Period 1987–2018, *Atmosphere*, 14, <https://doi.org/10.3390/atmos14030585>, 2023.
- Laube, J. C., Elvidge, E. C. L., Adcock, K. E., Baier, B., Brenninkmeijer, C. A. M., Chen, H., Droste, E. S., Groß, J.-U., Heikkinen, P., Hind, 465 A. J., Kivi, R., Lojko, A., Montzka, S. A., Oram, D. E., Randall, S., Röckmann, T., Sturges, W. T., Sweeney, C., Thomas, M., Tuffnell, E., and Ploeger, F.: Investigating stratospheric changes between 2009 and 2018 with halogenated trace gas data from aircraft, AirCores, and a global model focusing on CFC-11, *Atmospheric Chemistry and Physics*, 20, 9771–9782, <https://doi.org/10.5194/acp-20-9771-2020>, 2020.
- Laube, J. C., Schuck, T., Markus, H. C. G., van Heuven, S., Popa, T. K. M. E., Tuffnell, E., Vogelnd, B., Wagenhäuser, T., Zanchetta, A., 470 and Engel, A.: Vertical distribution of halogenated trace gases in the summer Arctic stratosphere determined by two independent in situ methods, *Egusphere*, 2024.
- Leedham Elvidge, E., Bönisch, H., Brenninkmeijer, C. A. M., Engel, A., Fraser, P. J., Gallacher, E., Langenfelds, R., Mühle, J., Oram, D. E., Ray, E. A., Ridley, A. R., Röckmann, T., Sturges, W. T., Weiss, R. F., and Laube, J. C.: Evaluation of stratospheric age of air from CF<sub>4</sub>, C<sub>2</sub>F<sub>6</sub>, C<sub>3</sub>F<sub>8</sub>, CHF<sub>3</sub>, HFC-125, HFC-227ea and SF<sub>6</sub>; implications for the calculations of halocarbon lifetimes, fractional release factors 475 and ozone depletion potentials, *Atmospheric Chemistry and Physics*, 18, 3369–3385, <https://doi.org/10.5194/acp-18-3369-2018>, 2018.
- Membrive, O., Crevoisier, C., Sweeney, C., Danis, F., Hertzog, A., Engel, A., Bönisch, H., and Picon, L.: AirCore-HR: a high-resolution column sampling to enhance the vertical description of CH<sub>4</sub> and CO<sub>2</sub>, *Atmospheric Measurement Techniques*, 10, 2163–2181, <https://doi.org/10.5194/amt-10-2163-2017>, 2017.
- NOAA: Sulfur Hexafluoride (SF<sub>6</sub>) WMO Scale, [https://gml.noaa.gov/ccl/sf6\\_scale.html](https://gml.noaa.gov/ccl/sf6_scale.html), accessed 21.10.2024, 2014.
- 480 Novelli, P. C., Steele, L. P., and Tans, P. P.: Mixing ratios of carbon monoxide in the troposphere, *Journal of Geophysical Research: Atmospheres*, 97, 20 731–20 750, <https://doi.org/10.1029/92JD02010>, 1992.
- Oakley, T., Vömel, H., and Wei, L.: WMO Intercomparison of High Quality Radiosonde Systems, Tech. Rep. WMO/TD-No. 1580, World Meteorological Organisation, Geneva, <https://library.wmo.int/idurl/4/50499>, 2011.
- Persson, C. and Leck, C.: Determination of Reduced Sulfur Compounds in the Atmosphere Using a Cotton Scrubber for Oxidant Removal 485 and Gas Chromatography with Flame Photometric Detection, *Anal. Chem.*, 66, 983—987, <https://doi.org/10.1021/ac00079a009>, 1994.



- Plumb, R. A. and Ko, M. K. W.: Interrelationships between mixing ratios of long-lived stratospheric constituents, *Journal of Geophysical Research: Atmospheres*, 97, 10 145–10 156, <https://doi.org/https://doi.org/10.1029/92JD00450>, 1992.
- Prinn, R. G., Weiss, R. F., Arduini, J., Arnold, T., DeWitt, H. L., Fraser, P. J., Ganesan, A. L., Gasore, J., Harth, C. M., Hermansen, O., Kim, J., Krummel, P. B., Li, S., Loh, Z. M., Lunder, C. R., Maione, M., Manning, A. J., Miller, B. R., Mitrevski, B., Mühle, J., O’Doherty, S.,  
490 Park, S., Reimann, S., Rigby, M., Saito, T., Salameh, P. K., Schmidt, R., Simmonds, P. G., Steele, L. P., Vollmer, M. K., Wang, R. H., Yao, B., Yokouchi, Y., Young, D., and Zhou, L.: History of chemically and radiatively important atmospheric gases from the Advanced Global Atmospheric Gases Experiment (AGAGE), *Earth System Science Data*, 10, 985–1018, <https://doi.org/10.5194/essd-10-985-2018>, 2018.
- Ray, E. A., Moore, F. L., Elkins, J. W., Hurst, D. F., Romashkin, P. A., Dutton, G. S., and Fahey, D. W.: Descent and mixing in the 1999–2000 northern polar vortex inferred from in situ tracer measurements, *Journal of Geophysical Research: Atmospheres*, 107, SOL 28–SOL  
495 28–18, <https://doi.org/https://doi.org/10.1029/2001JD000961>, 2002.
- Ray, E. A., Moore, F. L., Rosenlof, K. H., Davis, S. M., Sweeney, C., Tans, P., Wang, T., Elkins, J. W., Bönisch, H., Engel, A., Sugawara, S., Nakazawa, T., and Aoki, S.: Improving stratospheric transport trend analysis based on SF<sub>6</sub> and CO<sub>2</sub> measurements, *Journal of Geophysical Research: Atmospheres*, 119, 14,110–14,128, <https://doi.org/https://doi.org/10.1002/2014JD021802>, 2014.
- Ray, E. A., Moore, F. L., Elkins, J. W., Rosenlof, K. H., Laube, J. C., Röckmann, T., Marsh, D. R., and Andrews, A. E.: Quantification of the  
500 SF<sub>6</sub> lifetime based on mesospheric loss measured in the stratospheric polar vortex, *Journal of Geophysical Research: Atmospheres*, 122, 4626–4638, <https://doi.org/10.1002/2016JD026198>, 2017.
- Ray, E. A., Moore, F. L., Garny, H., Hintsa, E. J., Hall, B. D., Dutton, G. S., Nance, D., Elkins, J. W., Wofsy, S. C., Pittman, J., Daube, B., Baier, B. C., Li, J., and Sweeney, C.: Age of air from in situ trace gas measurements: Insights from a new technique, *EGUsphere*, 2024,  
1–32, <https://doi.org/10.5194/egusphere-2024-1887>, 2024.
- 505 Schmidt, U., Kulessa, G., Klein, E., Röth, E.-P., Fabian, P., and Borchers, R.: Intercomparison of balloon-borne cryogenic whole air samplers during the MAP/GLOBUS 1983 campaign, *Planetary and Space Science*, 35, 647–656, [https://doi.org/10.1016/0032-0633\(87\)90131-0](https://doi.org/10.1016/0032-0633(87)90131-0), 1987.
- Schuck, T. J., Lefrancois, F., Gallmann, F., Wang, D., Jesswein, M., Hoker, J., Bönisch, H., and Engel, A.: Establishing long-term measurements of halocarbons at Taunus Observatory, *Atmospheric Chemistry and Physics*, 18, 16 553–16 569, <https://doi.org/10.5194/acp-18-16553-2018>, 2018.  
510
- Schuck, T. J., Zanchetta, A., van Heuven, S., Degen, J., and Ghysels-Dubois, M.: Greenhouse gas profiles from the 2021 HEMERA-TWIN balloon launch, <https://doi.org/10.5281/zenodo.13918430>, 2024.
- Stiller, G. P., von Clarmann, T., Haenel, F., Funke, B., Glatthor, N., Grabowski, U., Kellmann, S., Kiefer, M., Linden, A., Lossow, S., and López-Puertas, M.: Observed temporal evolution of global mean age of stratospheric air for the 2002 to 2010 period, *Atmospheric  
515 Chemistry and Physics*, 12, 3311–3331, <https://doi.org/10.5194/acp-12-3311-2012>, 2012.
- Tans, P. P.: System and method for providing vertical profile measurements of atmospheric gases, US patent number 759701, 2009.
- Tong, X., Van Heuven, S., Scheeren, B., Kers, B., Hutjes, R., and Chen, H.: Aircraft-Based AirCore sampling for estimates of N<sub>2</sub>O and CH<sub>4</sub> emissions, *Environmental Science and Technology*, 57, 15 571–15 579, <https://doi.org/10.1021/acs.est.3c04932>, 2023.
- Vinković, K., Andersen, T., de Vries, M., Kers, B., van Heuven, S., Peters, W., Hensen, A., van den Bulk, P., and Chen, H.: Evaluating the  
520 use of an Unmanned Aerial Vehicle (UAV)-based active AirCore system to quantify methane emissions from dairy cows, *Science of The Total Environment*, 831, 154 898, <https://doi.org/https://doi.org/10.1016/j.scitotenv.2022.154898>, 2022.



- Volk, C. M., Elkins, J. W., Fahey, D. W., Dutton, G. S., Gilligan, J. M., Loewenstein, M., Podolske, J. R., Chan, K. R., and Gunson, M. R.: Evaluation of source gas lifetimes from stratospheric observations, *Journal of Geophysical Research: Atmospheres*, 102, 25 543–25 564, <https://doi.org/10.1029/97JD02215>, 1997.
- 525 Wagenhäuser, T., Engel, A., and Sitals, R.: Testing the altitude attribution and vertical resolution of AirCore measurements with a new spiking method, *Atmospheric Measurement Techniques*, 14, 3923–3934, <https://doi.org/10.5194/amt-14-3923-2021>, 2021.
- Wagenhäuser, T., Jesswein, M., Keber, T., Schuck, T., and Engel, A.: Mean age from observations in the lowermost stratosphere: an improved method and interhemispheric differences, *Atmospheric Chemistry and Physics*, 23, 3887–3903, <https://doi.org/10.5194/acp-23-3887-2023>, 2023.
- 530 Wagenhäuser, T., Engel, A., Bönisch, H., Ray, E., Garny, H., and Voet, F.: AtmosphericAngels/AoA\_from\_convolution: Software version as used in Garny et al. 2024, <https://doi.org/10.5281/zenodo.11127613>, 2024.
- Waugh, D. and Hall, T.: Age of Stratospheric Air: Theory, Observations, and Models, *Reviews of Geophysics*, 40, <https://doi.org/10.1029/2000RG000101>, 2002.
- WMO: GCOS - Essential Climate Variables, <https://gcos.wmo.int/en/essential-climate-variables/ghg/>, accessed 10.9.2024, 2024.
- 535 Zhou, M., Langerock, B., Vigouroux, C., Sha, M. K., Ramonet, M., Delmotte, M., Mahieu, E., Bader, W., Hermans, C., Kumps, N., Metzger, J.-M., Dufлот, V., Wang, Z., Palm, M., and De Mazière, M.: Atmospheric CO and CH<sub>4</sub> time series and seasonal variations on Reunion Island from ground-based in situ and FTIR (NDACC and TCCON) measurements, *Atmospheric Chemistry and Physics*, 18, 13 881–13 901, <https://doi.org/10.5194/acp-18-13881-2018>, 2018.